Published in final edited form as:
Proc SPIE. 2011 March 9; 7963: 79632A–79632A-6. doi:10.1117/12.878249.

Estimation of Myocardial Volume at Risk from CT Angiography

Liangjia Zhu[a], **Yi Gao**[b], **Vandana Mohan**[a], **Arthur Stillman**[c], **Tracy Faber**[c], and **Allen Tannenbaum**[a,b]

[a] School of Electrical & Computer Engineering, Georgia Institute of Technology, Atlanta GA 30332

[b] Department of Biomedical Engineering, Georgia Institute of Technology, Atlanta GA 30332

[c] Department of Radiology, Emory University, Atlanta, GA, 30322

Abstract

The determination of myocardial volume at risk distal to coronary stenosis provides important information for prognosis and treatment of coronary artery disease. In this paper, we present a novel computational framework for estimating the myocardial volume at risk in computed tomography angiography (CTA) imagery. Initially, epicardial and endocardial surfaces, and coronary arteries are extracted using an active contour method. Then, the extracted coronary arteries are projected onto the epicardial surface, and each point on this surface is associated with its closest coronary artery using the geodesic distance measurement. The likely myocardial region at risk on the epicardial surface caused by a stenosis is approximated by the region in which all its inner points are associated with the sub-branches distal to the stenosis on the coronary artery tree. Finally, the likely myocardial volume at risk is approximated by the volume in between the region at risk on the epicardial surface and its projection on the endocardial surface, which is expected to yield computational savings over risk volume estimation using the entire image volume. Furthermore, we expect increased accuracy since, as compared to prior work using the Euclidean distance, we employ the geodesic distance in this work. The experimental results demonstrate the effectiveness of the proposed approach on pig heart CTA datasets.

Keywords

Myocardial volume at risk; geodesic distance on surface; contour extraction on surface

1. INTRODUCTION

Prognosis and treatment of coronary artery disease frequently require the determination of the myocardial volume at risk caused by coronary stenosis. A previous study[1] shows that the regional myocardial mass at risk depends on the shape and content of myocardium distal to the coronary artery occlusion, which has been commonly used to estimate the myocardial area at risk. In one work[2], 3D models of the coronary artery tree are aligned with the 3D epicardial surface of the left ventricle (LV) built from perfusion SPECT to estimate the anatomic area at risk. Then, the mass at risk is obtained under the assumption that myocardium has a uniform thickness. In another work[3], each tissue voxel is assigned to its nearest arterial branch to determine the dependent myocardial region using micro-CT images. In order to compute the coronary perfusion territories from CTA, Dijkstra's

Further author information: (Send correspondence to L. Z.) L.Z.: ljzhu@gatech.edu.

algorithm is used to associate a region with its closest coronary over the LV epicardial surface segmented offline[4].

However, much less work has been done for computing the myocardial volume at risk directly on the heart surfaces segmented from CAT imagery, rather than employing simplified models such as ellipsoids. The purpose of this study is to provide an efficient and general computational framework for estimating the myocardial volume at risk that can capture the individual myocardial variability. In this work, the relation between the myocardial mass at risk and the coronary artery occlusion is adopted as the basis for computation. In addition, a decomposition strategy is utilized to reduce the computational cost by first finding the regions at risk over the epicardial and endocardial surfaces, and then reconstructing the volume in between these regions as the approximation of the myocardial volume at risk.

2. METHODS

The overall procedure is shown in Figure 1, which includes the following steps: (1) heart surfaces and coronary arteries extraction; (2) myocardial risk region estimation; and (3) myocardial volume estimation. The first step is semi-automatic that requires only a few user interactions. The second and third steps are the key part of the overall framework, which are automatic. The details of each step are given in the following sections.

2.1 Heart Surfaces Segmentation and Coronary Arteries Extraction

This is a preprocessing step. For heart surfaces segmentation, an interactive active contour method[5] is applied with user specified seed points to extract the epicardial and endocardial surfaces. The segmented surfaces are triangulated and represented by triangle meshes.

Coronary arteries can be extracted using the same active contour method describe above by putting seed points at the distal branch of each coronary artery to avoid these seed points overgrow to aorta area. The centerline of each coronary artery is extracted using a Vascular Modeling Toolkit (VMTK)[6]. The extracted coronary arterial centerlines are represented by a tree structure. Given the location of a stenosis on the artery tree, we can classify all the points on the artery tree into two types based on whether the point is affected by the stenosis or not. Here, all the branch points distal to the stenosis are labeled as *affected* and assigned different index from that of *unaffected* points.

2.2 Estimation of Region at Risk on the Epicardial Surface

Since the extracted coronary centerlines do not lie exactly on the epicardial surface, projection is performed for each point on the centerlines by finding its closest point in terms of Euclidean distance on the epicardial mesh. Then, an efficient geodesic distance field computation method[7,8] is applied to the epicardial mesh using the projected arteries as source curves which define the zero set of the distance field. The key observation of this method is that the geodesic distance within a triangle on a mesh is a straight line, therefore we can virtually unfold these triangles in a common plane and propagate the distance field along straight lines through the so-called *windows* of each triangle edge. There are two types of sources, i.e. point source and line source that induce a set of *windows* on the edge of a triangle as shown in Figure 2. One advantage of this window formulation is that all computations can be done in the local coordinates defined by triangle $p_0p_1p_2$. Each window is described by a seven dimensional vector (*type*, *id*, b_0, b_1, d_0, d_1, *dir*), where *type* is either point or line source, *id* is the index of the source, b_0 and b_1 specify the endpoints of a window, d_0 and d_1 are the distance from a window endpoints to their closest source *S*, and *dir* shows from which side of *x-axis* that the source *S* propagates. Starting from the source

curves, the distance information is propagated from one triangle to its neighbors in a Dijkstra-like manner (see[7,8] for details). A list of *windows* is maintained for each edge of a triangle to record the geodesic distance information for points in each window. After the distance field is computed over all triangles, each point on a triangle edge will be associated with its closest point on the source curves, i.e. coronary arteries. Then, the region at risk caused by a stenosis is defined as the region in which all its inner points associated with the affected artery points.

2.3 Volume at Risk Estimation

Correspondingly, we can define the likely region at risk on the endocarial mesh as the projection of the risky region of the epicaridal mesh onto the endocardial mesh. Then, the likely volume at risk can be approximated by the volume defined in between those two regions. In order to reduce computational cost, we proposed an efficient method to find the volume at risk. The method consists of four steps: (a) extract the outer contour of the region at risk on the epicardial mesh; (b) project the contour onto the endocardial mesh; (c) find the region within the projected contour as the region at risk on then endocardial mesh; (d) construct the volume in between these two regions and compute its value.

Specifically, in step (a), a new contour extraction method is proposed to handle the challenges in processing noisy epicardial surface in which classical contour following methods may fail. This method formulates contour following as a distance propagation problem. First, for points on the epicardial mesh, the potential boundary points are selected as those that have the same geodesic distance to both affected and unaffected artery points. Moreover, the neighborhood is defined for each potential boundary point as the set of boundary points that lie on its adjacent triangles on the epicardial mesh. Then, from an initial point, e.g. a stenosis point, we can take one of its neighboring points each time as the second propagation point and propagate the distance field among all these potential boundary points using Dijkstra's algorithm[9]. In each iteration, we can get one shortest path via backtracking the distance field from the farthest point to the start point. Finally, the longest shortest path is chosen as the contour for the region at risk. Ideally, a closed contour will be returned assuming the contour of the region at risk is not self-intersecting, which is a general case from our empirical observations. Unlike the classical contour following algorithms that need backtracking or even fail due to their local search characteristics for the next expansion direction, the proposed method has a global sense in that the shortest path is obtained only after the distance field has expanded through all the potential boundary points. A simulated example is given in Figure 3. There are three segments of simulated arteries, one of which is affected by a stenosis, denoted by S_0 in red color. The enlarged view of the mesh around S_0 is shown on the top left corner, where n_1 and n_2 are the neighbors of S_0. In this case, two iterations are needed, i.e. from direction $\overrightarrow{S_0n_1}$ or $\overrightarrow{S_0n_2}$. Two shortest path, c_1 and c_2, were returned by our method, and the longest one was selected as the final result, which is a directed curve.

After obtaining the outer contour, projection is performed for each of the contour point by finding its closest point on the endocardial mesh in terms of Euclidean distance. If the projections of two adjacent points do not share a common triangle, then the contour between these two projected points is interpolated by searching for the shortest path between those two points using Dijkstra's algorithm on the endocardial mesh. The classical flood fill algorithm is used to fill in the region within the projected contour defined in same the direction as the original contour.

Finally, the two regions at risk are linked by triangulating the area between the original and projected contours to form a closed volume which is taken as the approximation of the

myocardial volume at risk. The triangle vertices of the risk volume are ordered so that the normal of each triangle is consistent with others and the value of this volume is computed as[10,11]

$$V=\frac{1}{6}\sum_{k=1}^{F} g_k \cdot N_k,$$

where F is the number of triangles of the constructed volume, $g_k=(x_k^1+x_k^2+x_k^3)/3$ and $N_k=\overrightarrow{x_k^1x_k^2} \wedge \overrightarrow{x_k^1x_k^3}$ for the kth triangle with its three vertices as x_k^1, x_k^2, x_k^3.

The four key steps for estimating the volume at risk are summarized are shown in Figure 4.

2.4 Validation

Seven female pigs first underwent normal resting positron emission tomography (PET) Rb-82 imaging, and one week later underwent coronary catheterization and microembolization of either the distal left anterior descending (LAD) or left circumflex artery (LCx) coronary artery bed. A stent was placed at the site of microembolization as a marker that could be visualized in the CT. Pigs then underwent resting Rb-82 PET imaging and 64-slice dual-source CTCA using separate scanners. The CTCA were processed as described above, using the stent as the location of arterial “stenosis”. The PET scans were processed using a standard quantification program[12] to determine the mass of myocardium which was abnormal in the second study. This area is that which was supplied by the artery distal to the stent location, and thus, suffered embolization. We compared this mass at risk determined from PET to that computed from the CT anatomy alone. Both the absolute myocardial mass at risk and the percentage of mass at risk over the LV mass were compared.

3. EXPERIMENTAL RESULTS

The proposed approach has been validated with the pig CTA datasets described above. For our implementation, 3D Slicer3.6[13] was used to segment heart surfaces and extract coronary arteries since it has integrated the methods described in section 2.1. Moreover, the extracted coronary centerlines were down-sampled with a uniform step to get a concise representation. Figure 5 shows one segmentation of the left ventricular epicardial surface, endocardial surface, and coronary arteries, superimposed with CTA volume. One example of the estimated volume at risk with LCx occlusion is shown in Figure 6 with two different views.

In order to evaluate the accuracy of the proposed approach, we compared the myocardial mass at risk estimated from seven pig CTA datasets with their corresponding values determined from PET. The myocardial mass is computed assuming a uniform gravity of myocardium as 1.05g/mL. Both the absolute myocardial mass at risk and the percentage of mass at risk over the LV mass were compared. Results are shown in Table 1. Overall, the average error for the estimated absolute myocardial mass at risk is -1.6 ± 4.1g, and the average error for the percentage of mass at risk over the LV mass is $2\% \pm 5.4\%$, which show that the estimation accuracy of our approach is very close to that obtained from the PET datasets.

4. CONCLUSIONS AND FUTURE WORK

In this work, we propose a new computational framework for estimating the myocardial volume at risk caused by stenosis from CTA imagery using image processing and computational geometry techniques. We approximate the myocardial volume at risk as the volume in between the region at risk on the epicardial surface and its counterpart on the endocardial surface. This significantly reduces the computational complexity as compared to working on entire image volume directly. The experiments have shown good results and in future work, we will improve the accuracy of the heart surfaces segmentation, and make the overall framework works more automatically. Moreover, we will test our approach with human CTA and PET datasets to further evaluate its accuracy and potential application in actual human heart risk assessment.

Acknowledgments

This work was supported in part by grants from NSF, AFOSR, ARO as well as by a grant from NIH (NAC P41 RR-13218) through Brigham and Women's Hospital. This work is part of the National Alliance for Medical Image Computing (NA-MIC), funded by the National Institutes of Health through the NIH Roadmap for Medical Research, Grant U54 EB005149. Information on the National Centers for Biomedical Computing can be obtained from http://nihroadmap.nih.gov/bioinformatics. This work was also funded in part by NIH Grant No. R01 HL085417. Dr. Faber receives royalties from the sale of the Emory Cardiac Toolbox and has equity positions in Syntermed, Inc., which markets both ECTb and the Emory Reconstruction Toolbox. ECTb was used to process some of the data in this manuscript. The terms of this arrangement have been reviewed and approved by Emory University in accordance with its conflict of interest policies.

References

1. Seiler C, Kirkeeide RL, Gould KL. Measurement from arteriograms of regional myocardial bed size distal to any point in the coronary vascular tree for assessing anatomic area at risk. Journal of the American College of Cardiology. 1993; 21(3):783–97. [PubMed: 8436762]
2. Faber TL, Santana C, Garica EV, Candell-Riera J, Folks R, Peifer J, Hoppers A, Aguade S, Angel J, Klein J. Three-Dimensional fusion of coronary arteries with myocardial perfusion distributions: clinical validation. Journal of Nuclear Medicine. 2004; 45:745–753. [PubMed: 15136621]
3. Le H, Wong JT, Molloi S. Estimation of regional myocardial mass at risk based on distal arterial lumen volume and length using 3D micro-CT images. Computerized Medical Imaging and Graphics. 2008; 32(6):488–501. [PubMed: 18595659]
4. Beliveau P, Setser RM, Cheriet F, White RD, O'Donnell T. Computation of coronary perfusion territories from CT angiography. Computers in Cardiology. 2007; 34:753–756.
5. Gao, Y.; Tannenbaum, A.; Kikinis, R. Simultaneous multi-object segmentation using local robust statistics and contour interaction. MICCAI 2010 Workshop on Medical Computer Vision;
6. http://www.vmtk.org
7. Surazhsky V, Surazhsky T, Kirsanov D, Gortler S, Hoppex H. Fast exact and approximate geodesics on meshes. ACM SIGGRAPH. 2005:553–560.
8. Bommes D, Kobbelt L. Accurate Computation of Geodesic Distance Field for Polygonal Curves on Triangle Meshes. VMV. 2007:151–160.
9. Dijkstra EW. A note on two problems in connexion with graphs. Numerische Mathematik. 1959; 1:269–271.
10. Desbrun M, Meyer M, Schröder P, Barr AH. Implicit fairing of irregular meshes using diffusion and curvature flow. ACM SIGGRAPH. 1999:317–324.
11. Zhang C, Chen T. Efficient feature extraction for 2D/3D objects in mesh representation. ICIP. 2001; 3:935–938.
12. Garcia EV, Faber TL, Cooke CD, Folks RD, Santana C. The increasing role of quantification in clinical nuclear cardiology, the Emory approach. Journal of Nuclear Cardiology. 2007; 14:42–432.
13. http://www.slicer.org

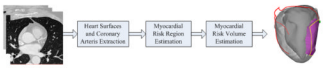

Figure 1.
The flowchart of the proposed framework.

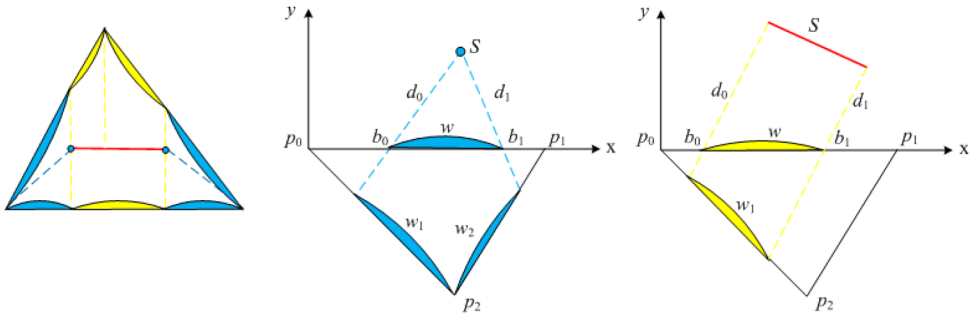

Figure 2.
Left: Windows induced by point sources (blue) and line source (yellow); Middle: Point source induced window propagation; Right: Line source induced window propagation.

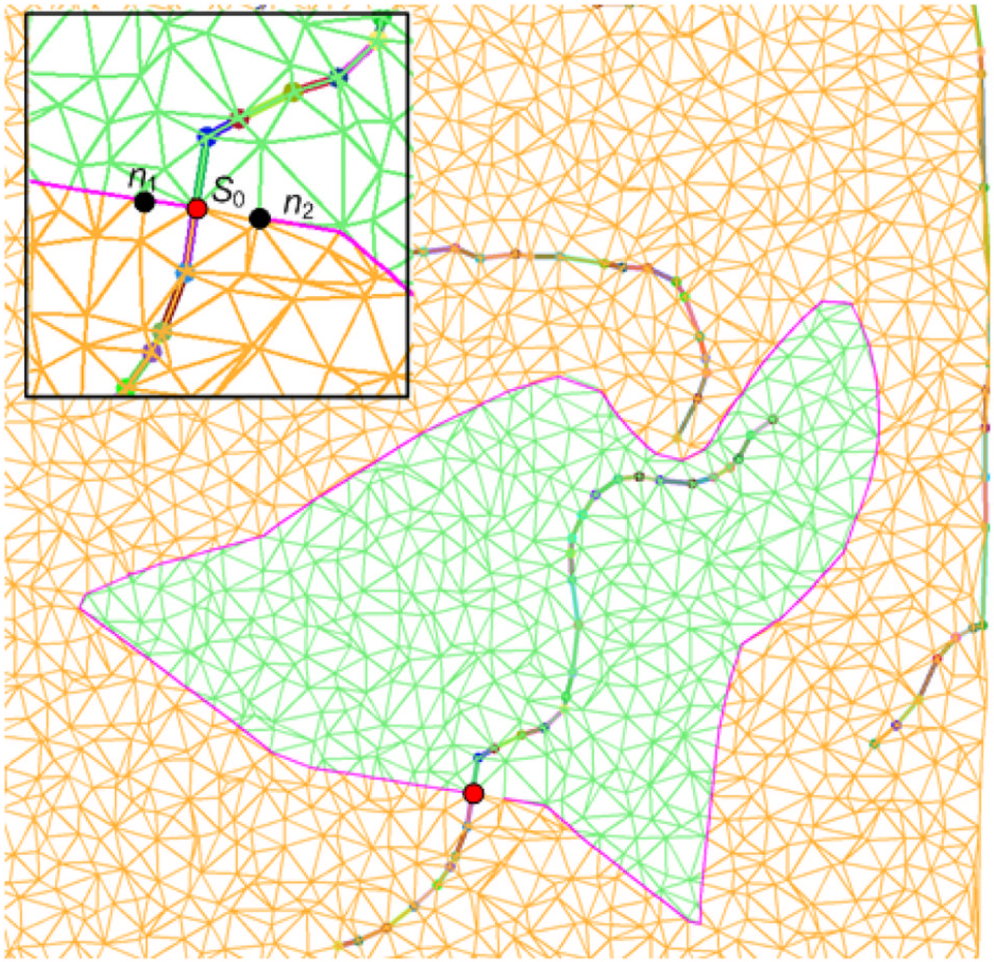

Figure 3.
An example of extracting the contour of region at risk. The extracted contour is marked with pink color.

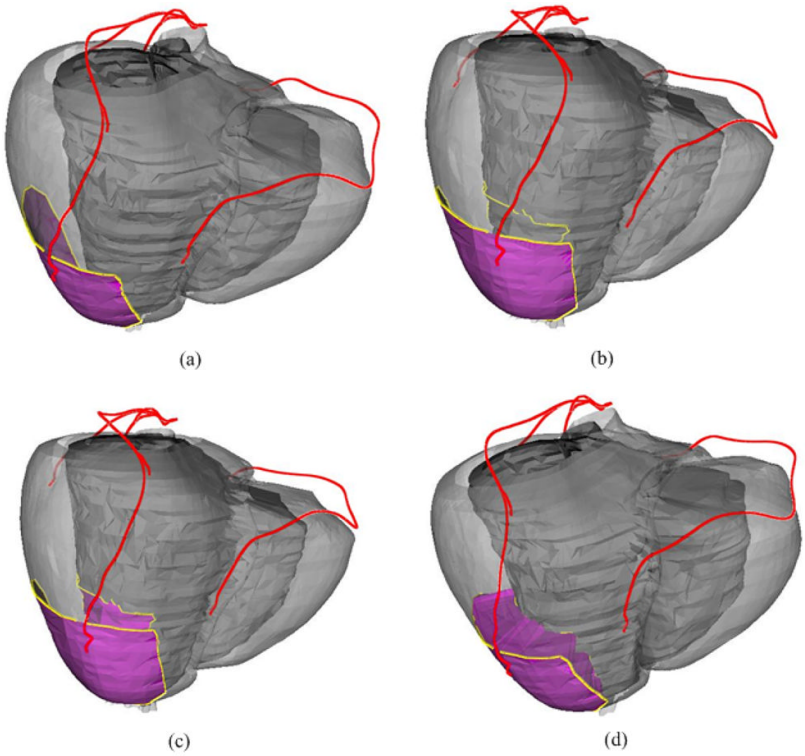

Figure 4.
An illustration of the process of estimating the myocardial volume at risk. (a) Contour of region at risk (yellow). (b) Projected contour on the endocardial mesh. (c) Region at risk on the endocardial mesh. (d) Approximated myocardial volume at risk.

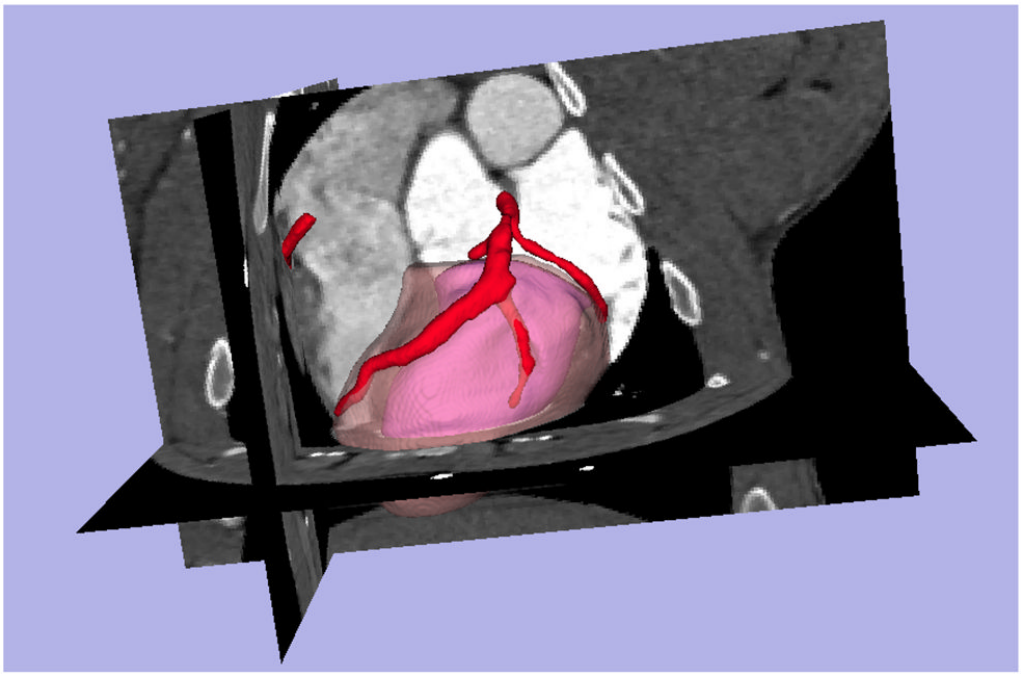

Figure 5.
Segmentation of left ventricular epicardial and endocardial surfaces, and coronary arteries. The epicardial surface is shown in a transparent model for a better visual effect.

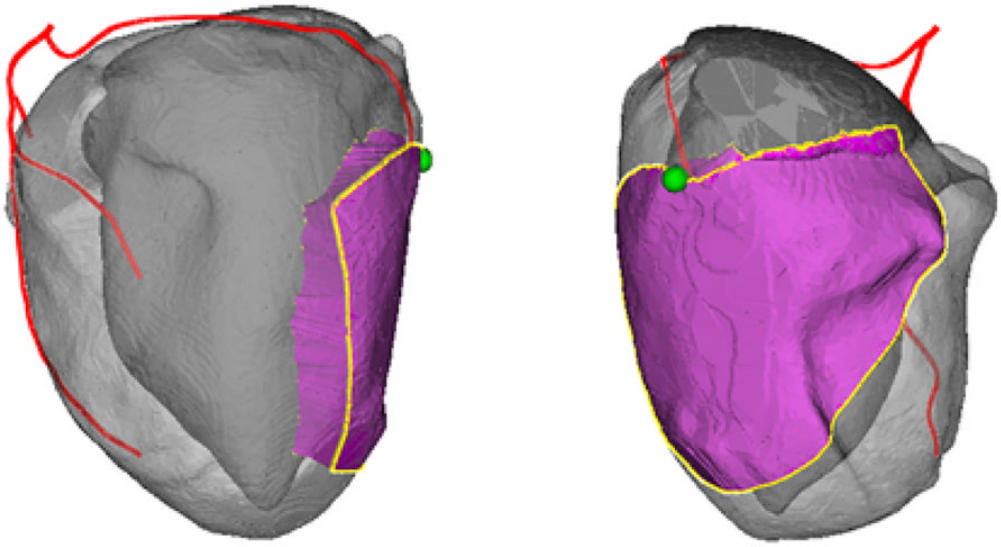

Figure 6.
Estimated myocardial volume at risk with LCx stenosis. Two views are shown, including the epicardial surface (light gray with transparency), endocardial surface (dark gray), coronary arteries centerlines (red), contour of regions at risk (yellow), and volume at risk (pink).

Table 1

Comparison of the myocardial mass estimated using our approach from CTA and that obtained from PET.

Pigs	Estimated Mass (g)	PET Mass (g)	Estimated %LV (%)	PET %LV (%)
Polly	14	16	23	19
Quinn	18	24	25	29
Ursula	12	16	17	19
Rosie	24	20	28	20
Tracy	20	16	25	16
Tammy	18	23	22	26
Velma	15	17	23	20